Raman Spectroscopy hyperspectral imager based on Bragg Tunable Filters

S. Marcet[*], M. Verhaegen[*], S. Blais-Ouellette[*], and R. Martel[**]

[*]Photon etc., 5795 Avenue de Gaspé, Montréal, Québec H2S 2X3, Canada, sbo@photonetc.com
[**] Département de chimie, Regroupement Québécois sur les Matériaux de Pointe (RQMP), Université de Montréal, Montréal, Québec H3C 3J7, Canada

ABSTRACT

A new type of Raman spectroscopy hyperspectral imager based on Bragg tunable filter has been developed by University of Montreal and Photon etc. The technology of Bragg tunable filter significantly reduces the acquisition time by selecting a single wavelength in a full camera field and scanning the wavelength with a high efficiency. The transmission is continuously tunable over 400 nm range with a spectral resolution of 0.2 nm. We here present the principle of this novel Raman imaging system as well as hyperspectral images of a Si/Ti structured wafer and carbon nanotubes taken with a spectral resolution of 0.2 nm on the whole field of view of the microscope.

Keywords: Raman imaging, Bragg tunable filter, hyperspectral

1 INTRODUCTION

Raman spectroscopy imaging simultaneously identifies and localizes a number of molecular species because of Raman diffusion specificity. This allows for the characterization of vibrational, optical and electronic properties that are difficult to observe with other measurement techniques. Raman spectroscopy requires maximum measurement efficiency because the signal from Raman diffusion is much weaker than other optical characterization techniques.

A new type of Raman spectroscopy imager has been developed by University of Montreal and Photon etc. The patented technology of the Bragg Tunable Filter (BTF) significantly reduces the acquisition time compared to currently available imagers [1] while keeping high spatial and spectral resolutions. The standard methods, point-to-point measurements or imagers using liquid crystal tunable filters, increase substantially the acquisition time because of the downtime of mechanical displacements of the sample or the low filter transmission and polarization sensitivity.

With a BTF, a single wavelength is detected at a time simultaneously on the whole image. Wavelengths are scanned by changing the angle of incidence of the beam on the BTF. The decision to use spectral rather than spatial scanning saves in acquisition time. The BTF has an achievable efficiency up to 80%, allowing for non-destructive molecular analysis with high sensitivity. The transmission is continuously tunable over 400 nm range with a spectral resolution of 0.2 nm.

We first present the general concept of the Raman spectroscopy hyperspectral imager. In the second part, we describe in more details the BTF. Finally, we present the first results of hyperspectral Raman images using the BTF technology on carbon nanotubes.

2 BASIC CONCEPT

Figure 1 shows an optical scheme of the Raman spectroscopy hyperspectral imager. To ensure a homogenous illumination over the entire field of view of the microscope objective, a single mode laser beam passes through a custom beam shaping module. The laser is then brought to the microscope with an open-space system and sent through a dichroic mirror to a microscope objective.

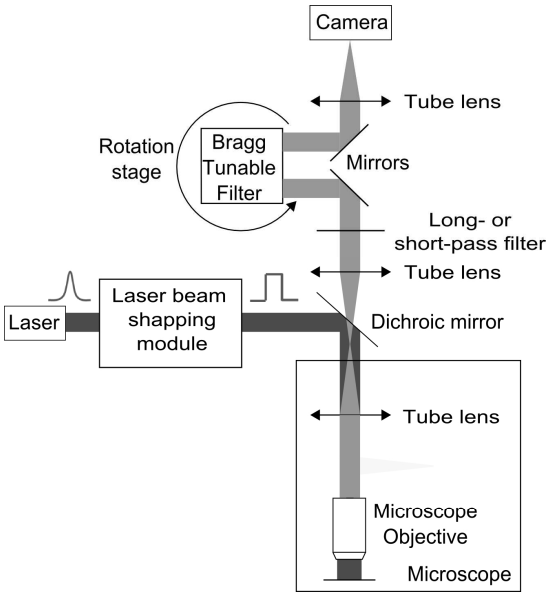

Figure 1 : Scheme of the Raman spectroscopy hyperspectral imager.

The light emitted from the sample is collected and collimated with the same objective, and transmitted through the dichroic mirror. A long- or short-pass filter, for Stokes or anti-Stokes scattering, respectively, suppresses the

Rayleigh diffusion and reflected laser light. Two tube lenses are used as a relay to image the pupil on the BTF.

A single wavelength of the whole image is filtered through the BTF where one resonant wavelength is diffracted and transmitted; other wavelengths are also refracted and split from the optical path. The filtered beam is then focalized by a tube lens on a charge-coupled device (CCD) camera, where a monochromatic image is formed. Wavelengths are scanned by changing the angle of incidence of the beam on the BTF.

3 DETAILS ABOUT THE FILTER

The filter is based on BTF technology that consists of a volume hologram in which the index of refraction varies periodically [2]. For a polychromatic collimated beam impinging on the volume hologram, only a particular narrow bandwidth will satisfy the Bragg condition and constructively interfere with the refractive index modulation, leaving other wavelengths non diffracted. Depending on the angle between the refractive index modulation and the direction of the incoming light, diffracted light will either be transmitted or reflected [3]. The resonant wavelength can be tuned over one hundred nanometers by changing the incident angle of the incoming light.

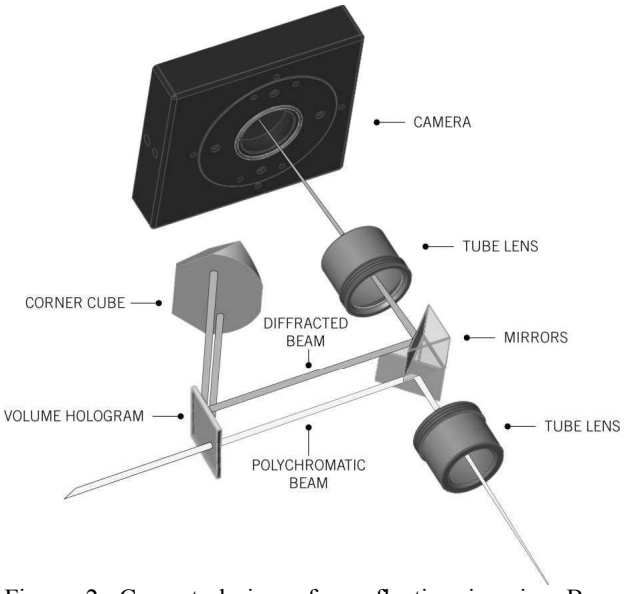

Figure 2. Current design of a reflection imaging Bragg tunable filter using a volume hologram.

Figure 2 shows a simplified design of the BTF. To ensure that the beam entirely passes through the volume hologram, the pupil of the optical system is imaged between the two grating passes by the first tube lens. The corner cube and the volume hologram are positioned on rotation stages to tune the diffracted wavelength. The non-resonant light passes through the grating, non diffracted. The diffracted beam is reflected and focused on a camera by another tube lens. The optical path within the filter has been carefully designed to almost eliminate the variations in the outcoming beam pointing. The tunability of the filter is accurate within 50 pm. With the aid of the internal calibration system, the filter can achieve this repeatable tuning precision over the full range.

The beam can be decomposed in a sum of collimated beams issued from different positions of the object seen by the microscope objective. Each collimated beam has a different incident angle on the volume hologram. The angular selectivity of the grating leads to a gradient in wavelength across the field of view in the dimension parallel to the dispersion axis (Figure 3). To get a monochromatic image, one would need to scan through a few wavelengths and retrieve the wavelength of interest for each image. This reconstruction is routinely done using PHOTON ETC. software.

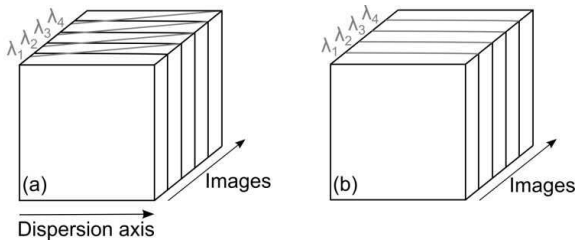

Figure 3. (a) Images with a gradient in wavelength in the dimension parallel to the dispersion axis and (b) reconstructed monochromatic images.

Volume hologram can reach diffraction peak efficiency of more than 90% (Figure 4). However, the diffraction efficiency has to be optimized for a given wavelength with the index modulation period and amplitude. The efficiency decreases for wavelengths apart from the maximum designed wavelength for *p*-polarized light while it slowly increases for *s*-polarized light. Figure 4(a) shows the calculated diffraction efficiency of a reflection volume hologram designed for a maximum wavelength of 633 nm. Due to optical path considerations, the incidence angle limits the diffracted wavelength between 500 to 600 nm. To achieve a larger wavelength scanning range with a high efficiency and narrow spectral bandwidth, four volume holograms are mounted on a rotating motorized stage, covering a bandwidth of 400 nm. They can be designed with a high efficiency from 400 to 2500 nm. Figure 4(b) shows the spectral response of the volume hologram used in the current set-up. It is designed to have a full width at half maximum of 0.2 nm. This narrow bandwidth is only achievable with thick reflection volume hologram. One can also note that the polarization sensitivity is important. However, this sensitivity may be decreased by optimizing the design parameters (index modulation period and

amplitude, and thickness) of the grating as it will be shown below.

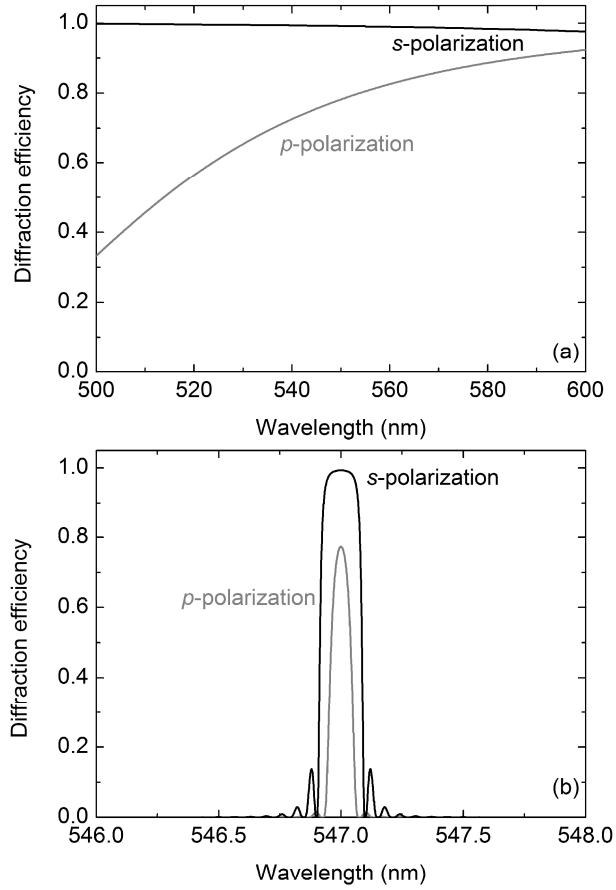

Figure 4. (a) Modeled diffraction efficiency for a reflection volume hologram for *s*- and *p*-polarization (black and grey lines, respectively). (b) Spectral response of the volume hologram centered at 547 nm.

4 PERFORMANCE

We have tested our imager with a Si substrate with a layer of carbon nanotubes. A pattern of Ti has been deposided above the carbon nanotubes. We use a single mode doubled Nd:YAG laser operating at 532 nm and a 20× microscope objective. The illumination area has a diameter of 250 µm. The power density on the sample is 250 $W \cdot cm^{-2}$.

Figure 5(a) shows an image at 532 nm, corresponding to the reflection of the laser. The long-pass filter has been removed to measure this image. The region 1 showing a higher reflectance is a structure of Ti material. The region 2 with a lower reflectance is the Si substrate where carbon nanotubes have been deposited. Figure 5(b) and (c) show images at 520 and 1580 cm^{-1} from the laser line, corresponding to the Raman diffusion of Si [4] and of the G band of carbon nanotubes [5], respectively. We clearly observe a signal emitted from the region 2 whereas no light is emitted from the region 1.

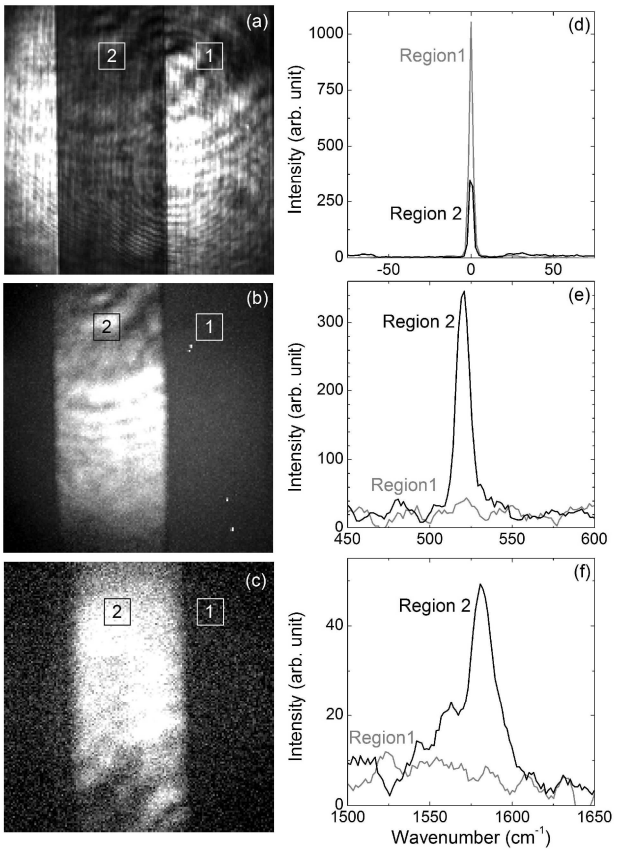

Figure 5. Monochromatic images at (a) 532 nm, (b) 520 cm^{-1} , and (c) 1580 cm^{-1} of a Si substrate with a pattern of Ti and a layer of carbon nanotubes. (d), (e), and (f) shows the spectra as a function of the wavenumber for the regions 1 and 2.

Figure 5(d) shows the local spectra at the laser wavelength from the regions 1 and 2. On Figures 5(e) and (f), the narrow peaks centered at 520 and 1580 cm^{-1} coming from the region 2 and the absence of light from the Ti pattern demonstrate that we observe the Raman diffusion from the Si substrate and carbon nanotubes with a spectral resolution of 7 cm^{-1}.

The Figure 5(b) and (c) have been measured from 542 to 550 nm and 577 to 585 nm, respectively, to compensate the gradient in wavelength. Then, the monochromatic images have been produced in few seconds using PHOTON ETC. reconstruction software.

The image of Figure 5(b) and (c) have been taken in 4 min (exposure time =3 s/image; wavelength step size=0.1 nm). However, several improvements are being made from the prototype we are currently using. First, the volume hologram used in this experiment was not specifically designed for Raman imaging and its size is twice smaller

than the pupil diameter. By using a larger volume hologram to match the pupil size, the intensity will increase by a factor of 4. Second, a better design will lead to higher diffraction efficiency and minimized polarization sensitivity. Figure 6 shows the calculated diffraction efficiency for a volume hologram designed for Raman spectroscopy imaging in the same wavelength range. Third, we are working on a better laser beam shaping which will help to obtain a more homogenous intensity across the image.

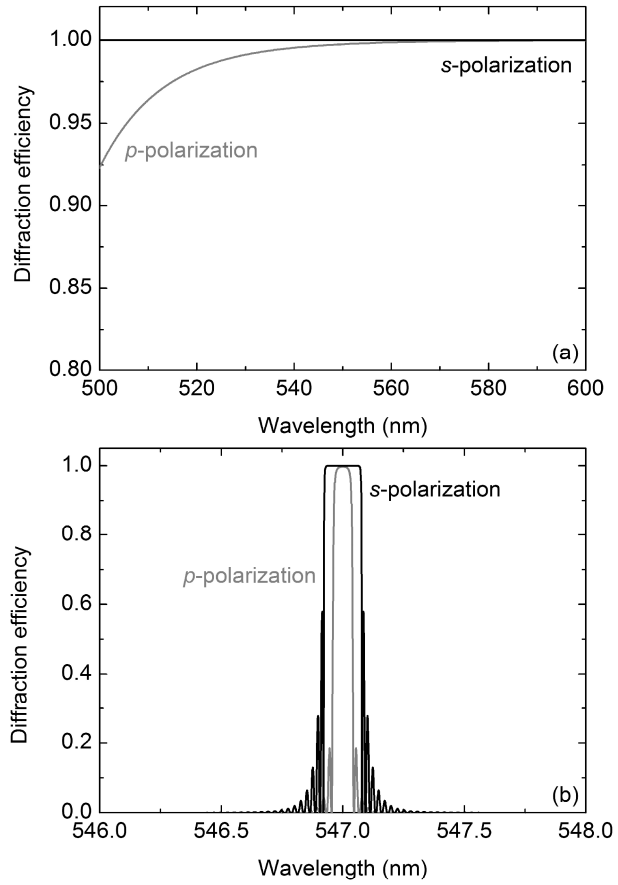

Figure 6. (a) Modeled diffraction efficiency for a reflection volume hologram for *s*- and *p*-polarization (black and grey lines, respectively). (b) Spectral response of the volume hologram centered at 547 nm.

Figure 7 shows the final design of the Raman spectroscopy hyperspectral imager. The laser beam shaping module and the BTF will be connected to a commercial upright microscope Olympus BX51 or inverted microscope Olympus IX71.

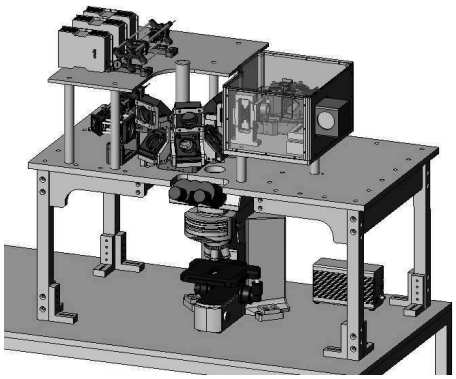

Figure 7. Final design of the Raman spectroscopy hyperspectral imager connected to a commercial upright microscope Olympus BX51.

5 CONCLUSION

A new type of Raman spectroscopy hyperspectral imager based on Bragg tunable filter has been developed and demonstrated. The imager is continuously tunable over 400 nm with a spectral resolution of 0.2 nm (<10 cm^{-1}) and an efficiency up to 80%. We have presented the first hyperspectral Raman images using the Bragg tunable filter technology on a Si/Ti structured wafer and carbon nanotubes. Several improvements are being made from the prototype we are currently using but we have shown that it is possible to use this technology for Raman spectroscopy imaging with the expected spectral resolution.

ACKNOWLEDGMENTS

This project is supported by NanoQuébec and the Natural Sciences and Engineering Research Council of Canada (NSERC).

REFERENCES

[1] A. Delamarre, "Mapping of quantitative photoluminescence spectra of solar cells," *SPIE Photonics West 2012*, 2012.

[2] S. Blais-Ouellette, "Method and apparatus for a Bragg grating tunable filter," US Patent 7,557,990, July 7, 2009.

[3] H. Kogelnik, "Coupled Wave Theory for Thick Hologram Gratings," *Bell Syst. Tech. J.*, vol. 48, p. 2909, 1969.

[4] J. H. Parker Jr., D. W. Feldman, and M. Ashkin, "Raman Scattering by Silicon and Germanium," *Phys. Rev.*, vol. 155, p. 712, 1967.

[5] M.S. Dresselhaus, "Raman spectroscopy of carbon nanotubes," *Physics Reports*, vol. 409, no. 2, p. 47, 2005.